6th International Conference on Advances in Experimental Structural Engineering
11th International Workshop on Advanced Smart Materials and Smart Structures Technology
August 1-2, 2015, University of Illinois, Urbana-Champaign, United States

Experimental Validation of a Large Capacity Semi-Active Friction Device

A. Downey[1], L. Cao[2], S. Laflamme[3], D. Taylor[4],J. Ricles[5]

1 *Research Assistant, Dept. of Civil, Construction and Environmental Engineering, Iowa State University, Ames, Iowa, United States. E-mail: adowney2@iastate.edu*
2 *Research Assistant, Dept. of Civil, Construction and Environmental Engineering, Iowa State University, Ames, Iowa, United States. E-mail: liangcao@iastate.edu*
3 *Professor, Dept. of Civil, Construction and Environmental Engineering, Iowa State University, Ames, Iowa, United States. E-mail: laflamme@iastate.edu*
4 *Chief Executive Officer, Taylor Devices, North Tonawanda, New York, United States. E-mail: taylordevi@aol.com*
5 *Professor, Dept. of Civil and Environmental Engineering, Lehigh University, Bethlehem, Pennsylvania, United States. E-mail: jmr5@lehigh.edu*

ABSTRACT
Implementation of high performance controllable damping devices can ameliorate cost-effectiveness of structural systems for mitigation of natural hazards. However, the applications of these damping systems are limited due to a lack of 1) mechanical robustness; 2) electrical reliability; and 3) large resisting force capability. To broaden the implementation of modern damping systems, a novel semi-active damping device is proposed. The device, termed Banded Rotary Friction Device (BRFD), has enhanced applicability compared to other proposed damping systems due to its cost-effectiveness, high damping performance, mechanical robustness, and technological simplicity. Its mechanical principle is based on a double wrap band brake, which results in a high amplification of the input force while enabling a variable control force. It is also possible to attach the BRFD in parallel with a stiffness element and a viscous damper to provide a fail-safe mechanism, analogous to the dynamics of magnetorheological dampers. Here, the BRFD is presented, and its principle demonstrated experimentally. The hysteresis of the friction force is characterized at low displacements and velocities. Results show that the BRFD is capable of friction forces up to 45 kN, making it a promising semi-active device for mitigation of natural hazards.

KEYWORDS: *variable friction; semi-active device; supplemental damping; structural control; modified friction device.*

1. INTRODUCTION

Passive supplemental damping systems have become widely accepted and installed in structures for their performance at natural hazard mitigation. However, their mitigation capability is typically limited to a bandwidth of excitations, which cannot be varied post manufacturing. Alternatively, active dampers provide higher mitigation performance, but they require large external power sources that may not be available during or after a natural hazard. Also, active systems have the potential to destabilize a system, and can be uneconomically to operate during sustained wind events (Connor, 2014).

Semi-active damping strategies combine many of the benefits of current passive and active systems. They typically perform over a large bandwidth of excitations provided by a variable damping mechanism, while providing pure reactive forces which requires low power to operate and prevents any possible destabilization of the controlled system. Semi-active devices are divided into four classes: variable stiffness (Liu, 2008); (He W, 2001), variable orifices (Yang J, 2007), variable fluid (SJ, 2004) and variable friction devices (BF Spencer Jr, 2003).

In particular, variable friction devices are capable developing high energy dissipation, independent on the velocity. Mechanical energy is dissipated into heat via a controllable normal force, which is modulated by means of an actuator. Existing examples of actuators and control schemes suitable for variable friction devices can be found in the literature, these include pneumatic; (Vesselenyi, 2007), electro-magnetic; (M. Lorenz, 2006), electro-mechanical; (S. Narasimhan, 2006), and piezoelectric; (Chaoqiang Chen, 2004). The ability to dynamically control the normal force minimizes many of the obstacles found in passive friction devices, namely the response produced by the strong nonlinear behavior, degradation of the sliding interface, and cold welds (MD Symans, 2008).

Several working examples of variable friction prototypes for structural control applications have been demonstrated in the literature. For instance, a semi-active, electromagnetic friction damper was proposed in (Anil K. Agrawal, 2000), which consists of one friction pad and two steel plates, with a demonstrated 20 kN (4.5 kips) maximum force. The normal force was adjustable by changing the electrical potential supplied to the plates. An independently variable semi-active friction device with a maximum damping force of 25 kN (5.5 kips), equipped by a electromechanical actuator has been demonstrated in (S. Narasimhan, 2006). This device utilizes stiffness elements in parallel with the friction dampers to act as restoring forces. More recently, investigations into a piezoelectric friction device with a damping capacity of 2.0 kN (0.5 kips) were conducted (Lu Lyan-Ywan, 2009). Implementation of semi-active friction devices in structural control applications have remained limited, despite studies demonstrating their economic benefits over passive systems, see references (Laflamme, 2011; Theodore L. Karavasilis, 2012; Yunbyeong Chae, 2013). Factors contributing to the low level of implantation could include the perceived low damping capability and the lack of mechanically reliable technologies of the available technologies (L Cao, 2015).

In an effort provide both high damping capacity and high mechanical reliability, a variable friction device based on existing band brake technology is introduced. This device, termed Banded Rotary Friction Device (BRFD), is designed to provide a high damping capacity based on a mechanically robust technology. A prototype of the BRFD is constructed and its dynamic behavior under various harmonic loads studied. The objective of this paper is to demonstrate the high damping potential of the novel semi-active device.

The paper is organized as follows. Section 2 introduces the BRFD and provides its theoretical background. Section 3 discusses the experimental methodology and the prototyping of the BRFD, and presents and discusses experimental results. Section 4 concludes the paper by providing a summary of the findings.

2. BANDED ROTARY FRICTON DEVICE

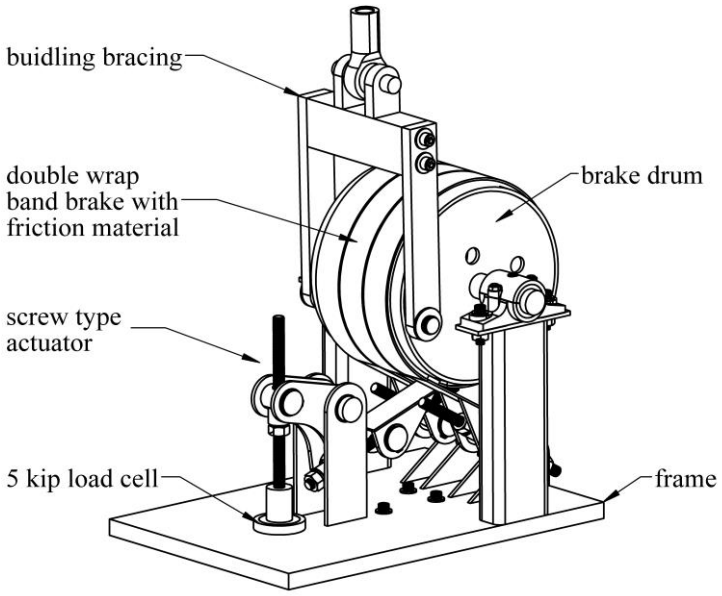

Figure 2.1 Banded rotary friction device

The BRFD is based on existing band brake technology. A band brake is a robust and reliable technology capable of providing dependable and predictable braking forces, having seen extensive use in the mining (United States Patent No. 1,353,370, 1920) and marine industries (Dong Seop Han, 2011). The BRFD consists of a band brake lined with a friction material, and doubled wrapped around a drum as shown in Figure 2.1. The device produces a variable braking torques as a linear function of the input force. This braking torque is significantly amplified by the band brake's positive servo effect.

A 45 kN (10 kips) capacity prototype was fabricated, with a band wrapped 670 degrees around a steel drum and anchored at both ends. One end of the band contains a screw type mechanical actuator, for the purpose of varying the force applied to the band brake. A load cell is placed under the actuator to measure the applied and reactionary forces.

2.1. Friction Mechanism

The damping force of the BRFD is a generated by the drum rotating through the stationary band; this interaction develops a friction force. The band is anchored at one end (called the slack end), where an input force (F_{applied}) is applied, resulting in a reactionary force (F_{reaction}) at the opposite end. When the drum experiences rotation, a friction force (F_{friction}) opposing the rotation of the drum is generated. This force causes the band to experience an equal force acting in the opposite direction. The forces acting on the band induces an elastic deformation and displacement in the direction of the drum rotation. As the tension in the band increases, starting where the application force was applied and towards the fixed end, the band wraps tightly around the drum, creating the self-energizing effect, also known as the positive servo effect. This phenomenon triggers an increases in the contact pressure of the friction material, increasing linearly with respect to the angular displacement from the point of the applied force on the drum (Baker, 1992). The contact pressure increases uniformly from zero at the F_{applied} end of the band, to its maximum value, located at the F_{reaction} end. For the mathematical model, it is assumed that the drum surface has a uniform curvature and that the band conforms evenly to the drum surface. The initial asymmetry due to manufacturing errors in the bands is not considered. The forces F_{applied}, F_{reaction} and F_{friction} can be related as follows. The relationship between the forces acting on the band ends (F_{applied} and F_{reaction}) is expressed as

$$\frac{F_{\text{reaction}}}{F_{\text{applied}}} = e^{\mu\phi} \tag{2.1}$$

where μ and ϕ represent the band wrap, expressed in radians and the friction materials friction coefficient, respectively. All forces acting on the band are in equilibrium, as shown in Eq. (2.2). Using the known relationship between F_{reaction} and F_{applied}, expressed in Eq. (2.1), Eq. (2.3) and Eq. (2.4):

$$F_{\text{reaction}} = F_{\text{friction}} + F_{\text{applied}} \tag{2.2}$$

$$F_{\text{reaction}} = \frac{F_{\text{friction}} \cdot e^{\mu\phi}}{(e^{\mu\phi} - 1)} \tag{2.3}$$

$$F_{\text{applied}} = \frac{F_{\text{friction}}}{(e^{\mu\phi} - 1)} \tag{2.4}$$

As shown in Eq. (2.2), the force F_{friction} is independent of the drum radius, r. The braking torque T can be expressed as $T = F_{\text{friction}} \cdot r$. The torque is used to generate a damping force F_{damping};

$$F_{\text{damping}} = \frac{T}{r_b} = \frac{F_{\text{friction}} \cdot r}{r_b} \tag{2.5}$$

From Eq. 2.5, the device‘s mechanical advantage C can be derived as:

$$C = \frac{F_{\text{damping}}}{F_{\text{applied}}} = \left(e^{\mu\phi} - 1\right) \cdot \frac{r}{r_b} \tag{2.6}$$

where $F_{\text{damping}} > F_{\text{applied}}$ (E. A. Vallone, 1996). The mechanical advantage C is a function of constants ϕ (expressed in radians), μ, r and r_b. It then follows that F_{damping} is a linear response of F_{applied} amplified by the constant C.

A schematic of the BRFD is shown in Figure 2.2, where forces w_1 and w_2 can act as either F_{applied} or F_{reaction}, determined by the direction of the drum rotation. This design allows for the damper to take full advantage of the positive servo effect in either directions of rotation. The BRFD is designed to sit on two support legs that produce opposite forces, shown here as F_{leg} that counteracts the moment produced by the forces acting on the drum, resulting in a zero moment gain, as experienced by the supporting substructure.

2.2. Laboratory Verification

The performance of the prototype BRFD at producing high damping forces was verified in a laboratory environment. The design parameters are listed in table 2.1. A picture of the prototype is shown in Fig. 2.3.

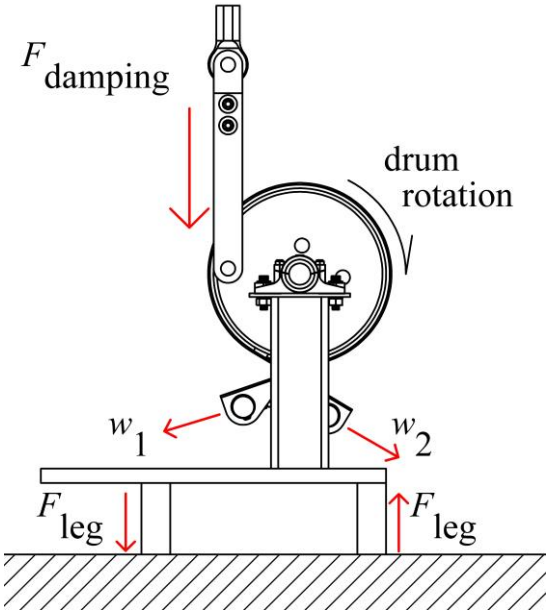

Figure 2.2 BRFD forces

Table 2.1 Validation of mechanical advantage

Parameter	Test value
Drum diameter	0.30 m (12 in)
Damping radius (r_b)	0.10 m (4 in)
Drum material	A-53 steel
Total band brake length	2.13 meters (84 in)
Band thickness	3.2 mm (1/8 in)
Coefficient of friction (μ)	0.39
Band brake wrap	670°
Mechanical advantage (C)	142

Figure 2.3 BRFD mounted in test setup

For validation purposes, the prototype BRFD was mounted in a servo-hydraulic testing machine. A load cell was placed under the screw activation mechanism for measuring the applied force and the reaction force upon reversal of the drum. The damping force generated was measured via a load cell located in the head of the testing machine. The test setup is shown in Figure 2.3, with the BRFD in its fully un-actuated position. The testing of the BRFD was limited to its designed 45 kN (10 kips) damping force capacity.

The prototype was subjected to a series of displacement-controlled harmonic excitations of 25.4 mm (1 in) amplitude at four different frequencies: 0.05, 0.1, 0.2, and 0.5 Hz. For each frequency, five different application forces $F_{applied}$ were investigated: 35 (8), 53 (12), 66 (15), 133 (30) and 267 N (60 lbs), where 35 N (8 lbs) is the minimum force available from the actuation mechanism and 267 N (60 lbs) corresponds approximately to the maximum capacity. In total, 20 tests were performed.

3. RESULTS

Figures 3.1 and 3.2 plot of the experimental data obtained from the dynamic testing, under 0.05 and 0.50 Hz excitations, respectively, and under varying levels of input forces (35, 53, 66, 133, and 267 N). A notable feature in the 0.50 Hz excitation data is a hump that occurs when the BRFD reverses, at the maximum force input (267 N) and less apparently at 133 N. The reduction in the damping force after the hump is likely due to slippage of the friction materiel that follows deviations in the brake band. Results show that the BRFD is capable of high damping force, in the order of 45 kN (10 kips).

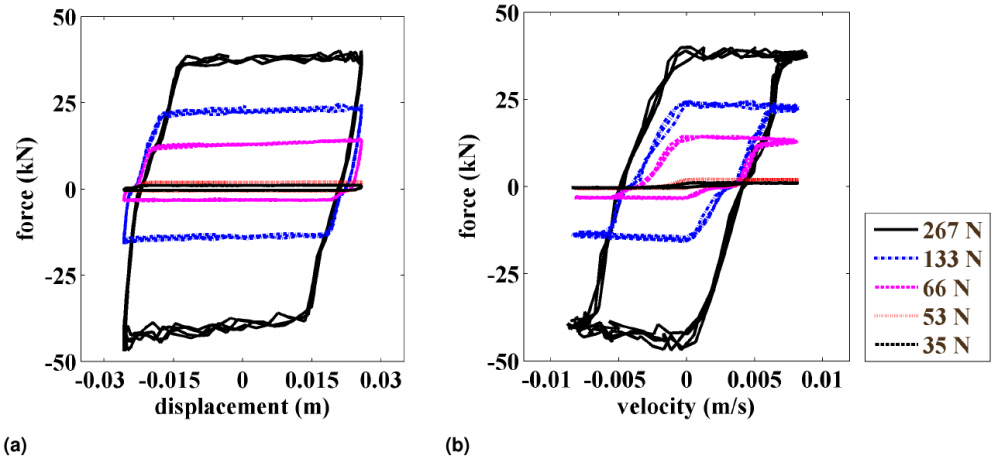

Figure 3.1 Experimental data fitting under various levels of force inputs for a 0.05 Hz excitation: (a) force-displacement; (b) force-velocity plots.

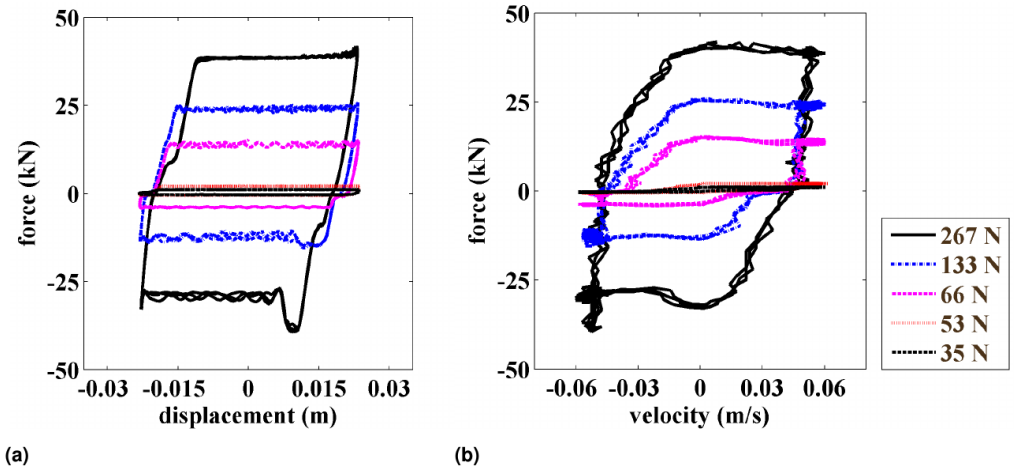

Figure 3.2 Experimental data fitting under various levels of force inputs for a 0.50 Hz excitation: (a) force-displacement; and (b) force-velocity plots.

Figure 3.3 compares the responses under various excitation frequencies under a constant input force (133N). Results are typical of other force inputs. The force-displacement loop remains approximatively constant under all excitation frequencies, with a slight decrease in the hysteresis at 0.5 Hz.

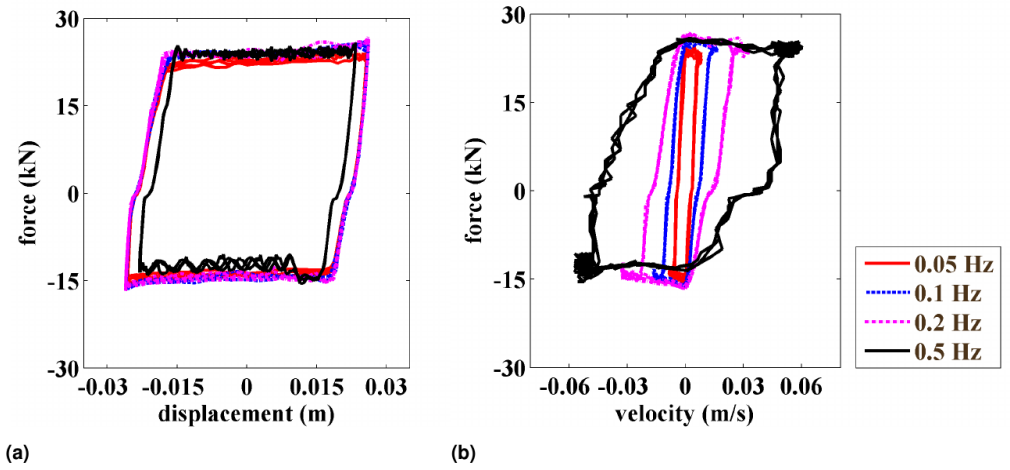

Figure 3.3. Experimental data fitting under various excitation frequencies for a 133 N (30 lbs) force input: (a) force-displacement; and (b) force-velocity plots.

3.1 Validation of Mechanical Advantage

The mechanical advantage C, derived in Eq. (2.6), can be directly calculated from the experimental data. To serve as a preliminary comparison with theory, it is best to use the values at the highest level of force input, for which the band brake is the tightest and its angle is the most constant. Table 3.1 list the C values for the forward rotation (C_{fwd}) and backward rotation (C_{bwd}) of the drum, along with the experimental coefficient of friction μ derived using Eq. (2.6) for both rotational directions. The experimental results show an agreement with design values. The lower C value for the backward rotation may be attributed to the asymmetries in the metal band and the adhered friction material.

Table 3.1 Validation of mechanical advantage

Parameter	Test value	Design value
C_{fwd}	145	142
C_{bwd}	126	142
μ_{fwd}	0.42	0.39
μ_{bwd}	0.41	0.39

4. CONSLUSION

In this paper, the authors have presented a novel variable friction damper for structural control applications. This device, termed Banded Rotary Friction Device (BRFD), is based on proven and efficient band brake technology. This technology has been leveraged to make the BRFD into a mechanically robust, semi-active damping system, which is capable of providing large and dependable damping forces, all while utilizing substantially lower force inputs due to the band brakes positive servo effect.

A prototype of the BRFD was fabricated and experimentally validated. The dynamic tests were conducted under harmonic loads at varying frequencies and application forces. Results show that the prototype BRFD is capable of obtaining a damping force of 45 kN (10 kips). The experimental value of mechanical advantage shows that the device was capable of a force amplification in the range of 125-150 times the applied force. These numbers showed agreement with theoretical values. The validated prototype and friction model presented in this research advances the potential for implementation of the semi-active friction device.

AKCNOWLEDGEMENT
This material is based upon work supported by the National Science Foundation under Grant no. 1300960. Their support is gratefully acknowledged. Any opinions, findings, and conclusions or recommendations expressed in this material are those of the authors and do not necessarily reflect the views of the National Science Foundation.

REFERENCES

1. Anil K. Agrawal, J. N. (2000). Semiactive control strategies for buildings subject to near-field earthquakes. Smart Structures and Materials 2000: Smart Systems for Bridges, Structures, and Highways, 359 (April 20, 2000), (p. SPIE 3988). Newport Beach.
2. Baker, A. K. (1992). Industrial brake and clutch design. London: Pentech Press.
3. BF Spencer Jr, a. S. (2003). State of the art of structural control. Journal of structural engineering, 845-856.
4. Chaoqiang Chen, G. C. (2004). Shake table tests of a quarter-scale three-storey building model with piezoelectric friction dampers. Structural Control and Health Monitoring, 239-257.
5. Connor, J.J., and Laflamme, S. (2014). Structural Motion Engineering. Springer.
6. Dong Seop Han, G. J. (2011). A Study on Durability Enhancement of Band Brake for Mooring Winch. Advanced Materials Research, Vol 201.
7. E. A. Vallone, T. B. (1996). Marks' Standard Handbook for Mechanical Engineers. New York: McGraw-Hill.
8. He W, A. A. (2001). Control of seismically excited cable-stayed bridge using resetting. Journal of Bridge Engineering, 376–384.
9. Jann N. Yang, J.-H. K. (2000). Resetting semiactive stiffness damper for seismic response control. Journal of Structural Engineering, 1427-1433.
10. Kawamoto, Y. (2008). Electro-mechanical suspension system considering energy consumption and vehicle manoeuvre. Vehicle System Dynamics, 1053-1063.
11. L Cao, A. D. (2015). Variable friction device for structural control based on duo-servo vehicle brake: Modeling and experimental validation. Journal of Sound and Vibration, 41-56.
12. Laflamme, S. (2011). Control of large-scale structures with large uncertainties. Diss. Massachusetts Institute of Technology.
13. Liu, Y. M. (2008). Semi-active vibration isolation system with variable stiffness and damping control. Journal of sound and vibration, 313(1), 16-28.
14. Lu Lyan-Ywan, G.-L. L. (2009). A theoretical study on piezoelectric smart isolation system for seismic protection of equipment in near-fault areas. Journal of Intelligent Material Systems and Structures, 217-232.
15. M. Lorenz, B. H. (2006). A novel engine mount with semi-active dry friction damping. Shock and Vibration, 559-571.
16. MD Symans, e. a. (2008). Energy dissipation systems for seismic applications: current practice and recent developments. Journal of Structural Engineering, 3-21.
17. S. Narasimhan, S. N. (2006). Smart base isolated buildings with variable friction systems: H∞ controller and SAIVF device. Earthquake engineering & structural dynamics, 921-942.
18. SJ, Y. O. (2004). Seismic control of a nonlinear benchmark building using smart dampers. Journal of engineering mechanics, 130(4): 386–392.
19. Theodore L. Karavasilis, R. S. (2012). Seismic design and evaluation of steel moment-resisting frames with compressed elastomer dampers. Earthquake Engineering & Structural Dynamics, 411-429.
20. Vesselenyi, T. (2007). Fuzzy and neural controllers for a pneumatic actuator. International Journal of Computers, Communications and Control 2.4, 375-387.
21. Williams, F. (1920). United States Patent No. 1,353,370.
22. Yang J, B. J. (2007). Full-scale experimental verification of resetable. Earthquake engineering & structural dynamics, 36(9): 1255–1273.
23. Yunbyeong Chae, J. M. (2013). Modeling of a large-scale magneto-rheological damper for seismic hazard mitigation. Part I: Passive mode. Earthquake engineering & structural dynamics, 669685.